Research Square

Preprints are preliminary reports that have not undergone peer review.
They should not be considered conclusive, used to inform clinical practice,
or referenced by the media as validated information.

Hidden Clues Within Blood: ATR-FTIR Spectroscopy and Chemometric Analysis for Determining the Ante-Mortem and Post-Mortem Origin of Blood

Sweety Sharma

Sharmasweety511@gmail.com

Manav Rachna International Institute of Research and Studies https://orcid.org/0000-0002-7886-4672

Mansi Patel

National Forensic Sciences University

Vijay Dhankar

Baba Saheb Ambedkar Hospital

Hirak Ranjan Dash

Centurion University of Technology and Management

Rajinder Singh

Punjabi University

Research Article

Keywords: Ante-mortem blood, post-mortem blood, Chemometrics, ATR-FTIR spectroscopy, Vibrational Spectroscopy, Biochemical Markers

Posted Date: August 14th, 2026

DOI: https://doi.org/10.21203/rs.3.rs-10693102/v1

License: This work is licensed under a Creative Commons Attribution 4.0 International License.
Read Full License

Additional Declarations: The authors declare no competing interests.

Hidden Clues Within Blood: ATR-FTIR Spectroscopy and Chemometric Analysis for Determining the Ante-Mortem and Post-Mortem Origin of Blood

Sweety Sharma*[*1], Mansi Patel[2], Vijay Dhankar[3], Hirak Ranjan Dash[4], Rajinder Singh[5]

[*1]School of Science, Manav Rachna University, Faridabad, Haryana, India

[*1]LNJN NICFS, School of Forensic Sciences, National Forensic Science University, An Institute of National Importance, Ministry of Home Affairs, Govt. of India, Delhi Campus, Delhi-110085-India

[2]LNJN NICFS, School of Forensic Sciences, National Forensic Science University, An Institute of National Importance, Ministry of Home Affairs, Govt. of India, Delhi Campus, Delhi-110085-India

[3]Department of Forensic Medicine, *Dr. Baba Saheb Ambedkar Hospital, Bhagawan Rohini, New Delhi, Delhi 110085*

[4]School of Forensic Sciences, Centurion University of Technology and Management, Bhubaneswar, Odisha, India-752050

[5]Punjabi University, Patiala, Punjab, 147002, India.

[*]**Corresponding Author**

Dr. Sweety Sharma,

Assistant Professor,

School of Science, Manav Rachna University, Faridabad, Haryana, India

Email ID: sharmasweety511@gmail.com

ORCID: 0000-0002-7886-4672

Abstract

The forensic identification and discrimination of various types of body fluids play a pivotal role in criminal investigations to determine how a crime has occurred. Over the years, several techniques have been employed to identify body fluids; however, Attenuated ATR-FTIR spectroscopy stands out as one of the most effective methods to analyse the biochemical properties of body fluids. The present study focuses on the use of ATR-FTIR

spectroscopy, in conjunction with multivariate statistical analysis, to discriminate between ante-mortem and post-mortem blood samples. In addition, the research extends to examine how different substrates may affect the detection of these blood samples. ATR-FTIR spectroscopy is a rapid and non-destructive analytical technique, and it facilitates the fingerprinting of biological fluids by analysing their unique biochemical composition through minimal or no sample preparation. The application of chemometric tools, such as PCA, PLS-DA, and LDA, facilitates the classification of ante-mortem and post-mortem blood samples. The present study demonstrates that the combined use of ATR-FTIR spectroscopy and chemometric analysis offers a rapid, non-destructive, and reliable approach for the forensic differentiation of antemortem and postmortem blood samples with 100% accuracy. The study further evaluates the influence of different substrates and storage conditions on blood analysis. Additionally, menstrual blood samples were incorporated as an external validation dataset, and the developed model successfully discriminated menstrual blood from ante-mortem and post-mortem blood samples with complete classification accuracy, thereby strengthening its forensic applicability in complex case scenarios.

Keywords: Ante-mortem blood, post-mortem blood, Chemometrics, ATR-FTIR spectroscopy, Vibrational Spectroscopy, Biochemical Markers

1. INTRODUCTION

Body fluids encountered at crime scenes serve as fundamental and essential evidence in forensic investigations, especially in cases involving physical violence such as assault, murder, and sexual assault [1]. Commonly collected body fluids include blood, semen, saliva, urine, vaginal secretions, and sweat, all of which play a critical role in examining crimes involving physical harm, including sexual assault and homicide. Among these, blood, if recovered, is considered the most significant biological fluid for crime scene analysis and reconstruction, as it offers valuable information for understanding the events. Distinguishing and identifying the type or origin of body fluids is crucial for providing insights into the alleged crime. Moreover, accurate determination of body fluid types can improve the quality of future DNA analysis, thereby aiding in the personal identification of individuals involved. Various presumptive and confirmatory procedures have been developed, primarily relying on immunological or enzymatic methods tailored to each body fluid. However, these approaches often require complex sample preparation, the use of

reagents or labels, and are susceptible to interference from other blood components. This adds to the overall costs associated with instrumentation, reagents, and analysis [2–5].

One of the principal challenges in forensic analysis arises when blood samples of similar appearance must be distinguished, particularly in situations where it is crucial to ascertain whether the blood is of ante-mortem or post-mortem origin. Determining whether blood loss occurred while the individual was still alive is of immense forensic significance. Such differentiation directly contributes to the assessment of wound vitality, the reconstruction of the sequence of events, and the formulation of cause-of-death opinions. Moreover, this distinction enables investigators to differentiate between true haemorrhage and post-mortem staining, which is also essential for accurate forensic interpretation. Additionally, identifying ante-mortem blood as opposed to post-mortem blood is critical, as this impacts the understanding of underlying pathology and influences the determination of the manner of death during medicolegal investigations [6,7].

Nowadays, various techniques are available to discriminate between ante-mortem and post-mortem blood based on morphological, immunochemical, and biochemical markers. Though these methods have an improved reliability, detectability of such techniques declines with post-mortem interval and decomposition. Morphological and histological examination, such as organised fibrin networks, factor XIIIa stabilisation, and serum-erythrocyte discontinuity, are indicative of the vital ante-mortem haemorrhage [6]. Kibayashi 1991, reported that Glycophorin A is detectable in true ante-mortem bleeding samples, and it was absent in post-mortem haemoglobin infiltration samples [8]. Post-mortem blood often shows much higher myoglobin which discriminates it from ante-mortem stains and also identifies the aged or putrefied post-mortem blood [9]. NADH and ammonia levels increased with post-mortem interval in comparative studies, and white blood cell degeneration progressed over hours to days, supporting timing assessments when combined with assays. However, there is insufficient evidence on any single gold-standard biochemical or morphological marker which reliably classifies all ante-mortem versus post-mortem blood across all contexts [10]. These conventional methods are often hindered by lengthy procedures, high costs, and the risk of inaccurate results, which can arise due to post-mortem biochemical alterations, microbial activity, and redistribution of substances within the body.

There is a need for an analytical system capable of detecting biochemical elements in ante-mortem and post-mortem blood samples. Attenuated Total Reflectance-Fourier Transform Infrared (ATR-FTIR) spectroscopy provides a reagent-free, rapid, and non-destructive method for identifying a wide range of biochemical components in blood with minimal sample preparation. This makes ATR-FTIR spectroscopy advantageous for forensic applications.

Chemometrics, when combined with ATR-FTIR spectroscopy, enables the objective characterisation of blood samples and serves as a powerful analytical tool. The use of vibrational spectroscopy for trace characterisation is inherently non-destructive, making it suitable for forensic casework. Several studies have already employed infrared spectroscopy as a screening technique for evaluating body fluid samples [1,4,11–14].

There is published literature in which ATR FT-IR was explored to discriminate between ante-mortem and post-mortem blood samples. The effect of substrates, including polyester, cotton, and denim, was explored in this paper using a weighted linear regression approach with multivariate statistical modelling for signal extraction and discrimination [15]. Furthermore, the forensic discrimination of menstrual blood from ante-mortem and post-mortem blood remains largely unexplored, even though such differentiation carries substantial evidentiary value in crime scene reconstruction and sexual assault and infanticide cases. In addition, the effect of storage conditions and other complex substrates on the spectral characteristics of blood samples has not been explored.

The present study highlights the combined application of multiple chemometric techniques, such as Principal Component Analysis (PCA), Partial Least Squares–Discriminant Analysis (PLS-DA), and Linear Discriminant Analysis (LDA) for classification of ante-mortem and post-mortem blood. The study appears to focus more on direct spectral fingerprinting on substrates and statistical classification, potentially offering a comparatively simpler and more implementable forensic methodology. Furthermore, the study investigates the discrimination of ante-mortem and post-mortem blood from menstrual blood, which represents a critical forensic challenge due to their biochemical similarities and the possibility of misinterpretation at crime scenes. The present study also incorporates the effect of different storage conditions, including room temperature and −80°C preservation, on the spectral characteristics of blood samples.

2. MATERIALS AND METHODS

2.1 Sample Collection and Preparation

A total of 20 ante-mortem blood samples and 10 menstrual blood samples were collected from healthy volunteers after obtaining ethical approval from the Institutional Ethical Committee of the National Forensic Sciences University, Delhi Campus (Approval No. NFSU-DC/EC/005/2025). Before sample collection, informed written consent was obtained from all volunteers in accordance with established ethical guidelines.

Ante-mortem blood samples were collected using the finger-prick method with sterile safety lancets (Bio Point® Blood Lancets). Approximately 20 µl of blood from each donor was deposited directly onto clean glass slides without the addition of anticoagulants. The samples were subsequently allowed to dry at room temperature (25 ± 5 ºC) for 24 hours to ensure complete dehydration.

Menstrual blood samples were collected anonymously from volunteer donors using menstrual cups (Pee Safe Reusable Menstrual Cup for Women). Donors were instructed to wear the menstrual cup for approximately 6–7 hours, after which the collected samples were transferred into sterile containers and stored at −80 ºC until further analysis.

A total of 40 post-mortem blood samples were collected from the cardiac region of deceased individuals during medico-legal autopsies conducted at Dr Baba Saheb Ambedkar Hospital, Rohini, Delhi. These samples were collected only from bodies in which decomposition had not commenced, as clinically confirmed by the autopsy surgeon during medico-legal examination. Prior informed written consent was obtained from the deceased's next of kin before sample collection. The post-mortem blood samples were collected in EDTA vials to preserve sample integrity and stored at −80 ºC until use.

Before ATR-FTIR spectroscopic analysis, frozen post-mortem and menstrual blood samples were thawed to room temperature and gently mixed to ensure sample homogeneity. Subsequently, 20 µl of each sample was carefully deposited onto clean glass slides and allowed to air dry at room temperature (25 ± 5 ºC) for 24 hours. Following complete drying, the blood residues were gently scraped from the glass slides using a sterile spatula to avoid contamination and directly transferred onto the ATR crystal surface for analysis.

ATR-FTIR spectra of all samples were recorded in the spectral range of 4000–600 cm^{-1} using a spectral resolution of 4 cm^{-1}. Each sample was analysed in triplicate to ensure spectral reproducibility and reliability for subsequent chemometric analysis.

2.2 Substrate Study of Post-mortem Blood Stains

To assess the actual recovery of post-mortem blood stains from crime scenes, a comprehensive substrate study was conducted. The substrates selected for this study included cotton, fibres, hairs, and nails, which are commonly encountered at crime scenes. For the experimental procedure, sections of cloth materials measuring 3×3 cm were carefully cut. On each of these substrates, a small amount of post-mortem blood was deposited to simulate real-case conditions. The samples were then left to air-dry at room temperature for a period of 24 hours, ensuring that the blood stains had adequately set for subsequent analysis.

Following the drying process, the blood-stained substrates were placed directly onto the ATR crystal for analysis. Each sample underwent three scans at a resolution of 4 cm^{-1} over the spectral range of 4000–600 cm^{-1}, allowing for the acquisition of reproducible and reliable spectra for further examination. The spectral collection was carried out at (25 ± 5 ºC). The blank substrate was used to collect the background spectra.

2.3 Storage Condition

To investigate the effect of storage conditions on post-mortem blood samples, a set of five samples was analysed without being stored at -80 ºC. For this purpose, 20 µl aliquots of blood were collected from the cardiac region of deceased individuals and directly deposited onto clean glass slides without the use of any preservatives. All the samples were then allowed to air-dry at room temperature. After complete drying, the blood residues were carefully scraped from the glass slides using a sterile spatula to avoid contamination. Samples were also analysed after storing at -80ºC in an EDTA vial.

2.4 ATR-FTIR Instrumentation and Spectral Acquisition

The spectral analysis of the samples was carried out using an ATR-FTIR spectrometer (Bruker, Alpha II) equipped with a zinc selenide (ZnSe) crystal. For data acquisition Opus software (version 7.5) was used. Spectra were recorded in the mid-IR region, specifically within the spectral range of 4000–600 cm^{-1}, with a 4 cm^{-1} resolution. To maintain the integrity of the measurements and minimise cross-contamination, the ATR-FTIR crystal was cleaned during each sample analysis. Cleaning was performed using cleaning tissues

moistened with isopropyl alcohol, ensuring that the crystal surface remained free from residual materials between runs.

For the analysis of samples deposited on various substrates, a blank substrate was initially scanned to obtain the background spectrum. Subsequently, a post-mortem bloodstain applied to the same surface was analysed as the sample, permitting the identification of blood-specific spectral features by comparison to the substrate background.

2.5 Multivariate data analysis

Unscrambler X software was used to apply the multivariate data analysis. The data were saved as .dpt files and then imported into the Unscramble X software. The spectral information was analysed using PCA, PLS-DA, and LDA. The pre-processing methods and parameters are given in Table 1.

Table 1: Pre-processing methods for PCA, PLS-DA and LDA

Parameter	PCA Model	PLS-DA Model
Pre-processing Applied	Baseline Correction; Savitzky–Golay Smoothing	Baseline Correction; Deresolve Transformation
Smoothing	Savitzky–Golay	Not Applied
De-resolution	Not Applied	Applied
Mean Centering	Applied	Applied
Algorithm Used	Singular Value Decomposition (SVD)	Kernel Algorithm
Validation Method	Cross-validation	Cross-validation
Cross-validation Type	Random (20 segments)	Random (20 segments)
Total Components / Factors	7 Components	7 Factors

2.6 Model Validation

The parameters used in the validation study were false positive and negative rates, sensitivity, specificity and accuracy. The above parameters can be calculated using the given formulae [12].

Sensitivity = true positives/ (true positives + false negatives) × 100

Specificity = true negative/ (true negatives + false positives) × 100

Accuracy = true positive + true negative/ (true positive + true negative + false positive + false negative) × 100

Precision = true positive/ (true positive + false positive) × 100

False positive rate = false positive/ (true positive + false negative) × 100

False negative rate = false negative/ (true negative + false positive) × 100

Model validation was performed for two products, and the output was only 'post-mortem blood' or 'not'.

2.7 External Validation

A blind external validation study was performed to evaluate the robustness and predictive reliability of the developed chemometric model. For this purpose, menstrual blood samples were collected as an independent external dataset along with ante-mortem and post-mortem blood samples. A total of 10 samples from each class were analysed.

3. RESULTS AND DISCUSSION

3.1 Comparison of Ante-mortem and Post-mortem Blood Spectra

A visual inspection of spectra collected from five representative samples of both ante-mortem blood and post-mortem blood exhibits no significant differences among the individual donors within each group. The overlaid spectra presented in Figure 1 for the ante-mortem group and Figure 2 for the post-mortem group demonstrate a high degree of similarity among the respective samples. This consistency indicates that, within the groups of ante-mortem and post-mortem blood, the spectral characteristics remain largely uniform across different donors. The representative overlaid spectra for the five ante-mortem and five post-mortem blood donors are clearly depicted in **Figures 1 and 2,** respectively.

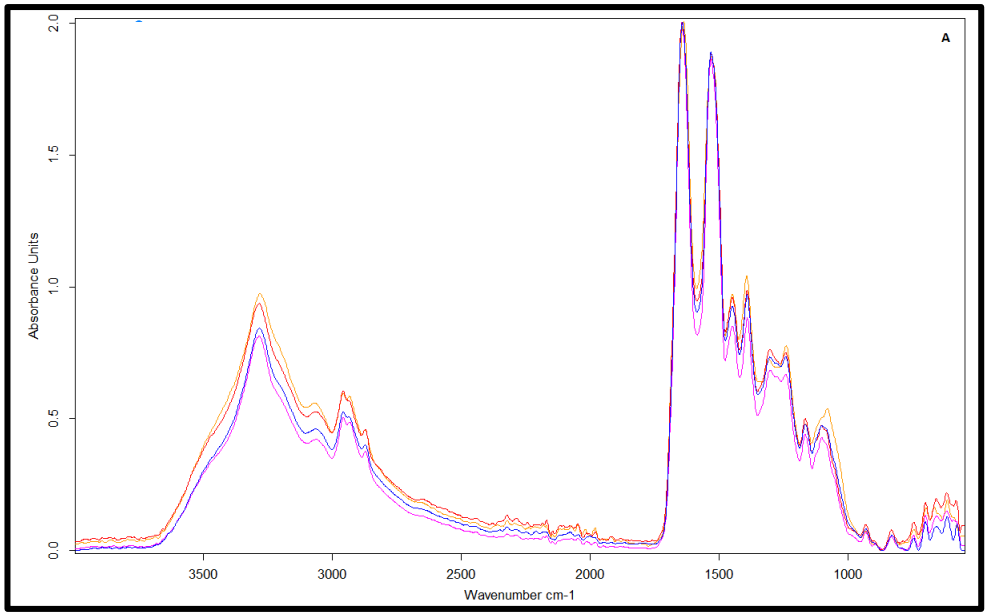


Fig. 1 Comparative ATR FT-IR spectra of neat Ante-mortem blood from different donors (represented by 5 individual donors)

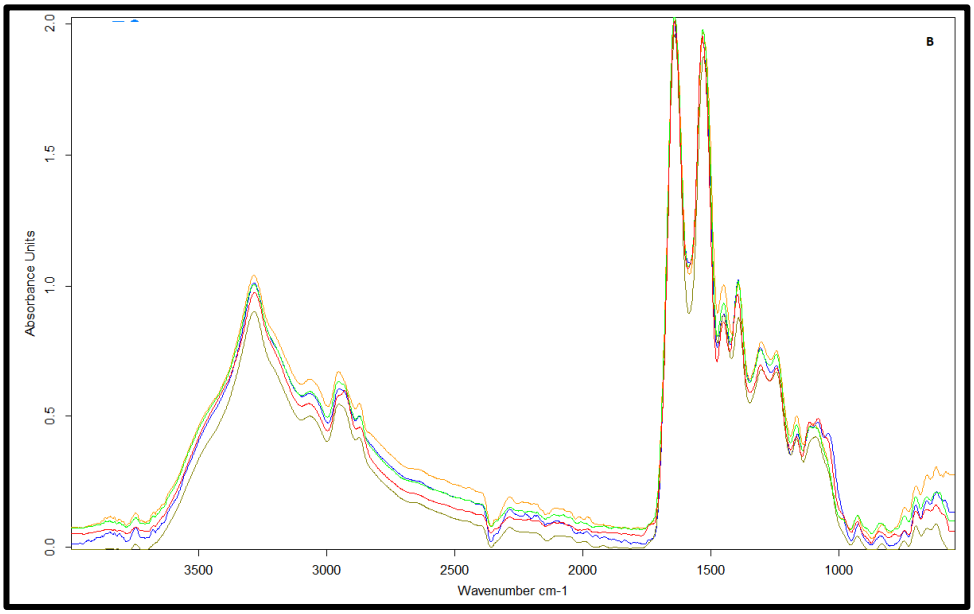


Fig. 2 Overlaid ATR FT-IR spectra of neat Post-mortem blood from different donors (represented by 5 individual donors)

3.2 Preliminary Visual discrimination of Ante-mortem and Post-mortem Blood

Fig. 3 illustrates the overlaid spectra of ante-mortem and post-mortem blood samples. The ATR FT-IR spectra for both types of blood appear substantially identical, with nearly matching absorbance values at corresponding wavenumbers. **Table 1** shows the vibrational functional groups in the ante-mortem and post-mortem blood samples [15].

Table 1 shows the vibrational functional groups in the ante-mortem and post-mortem blood samples [15]

Peak observed	**Wavenumber (cm^{-1})**	**Biomolecular Assignment**	**Functional Group / Vibration**	**Component**
~3283	3285	Amide A	N–H stretching	Protein
~2959	2959	Lipids	Asymmetric methyl (CH_3) stretching	Lipid
~2869	2873	Lipids	Symmetric methylene (CH_2) stretching	Lipid
~1639	1643	Amide I	C═O stretching	Protein
~1531	1532	Amide II	N–H bending and C–N stretching	Protein
~1459	1454	CH_3 bending (asymmetric)	Amino acid side chains	Proteins / Lipids
~1391	1392	CH_3 bending (symmetric)	Amino acid side chains	Proteins / Lipids
~1247	1241	Amide III	C–N stretching / N–H bending	Protein
~1165	1165	Lipids	C–O stretching of lipid ester	Lipid
~1083	1082	Glucose	Symmetric C–O stretching	Carbohydrate

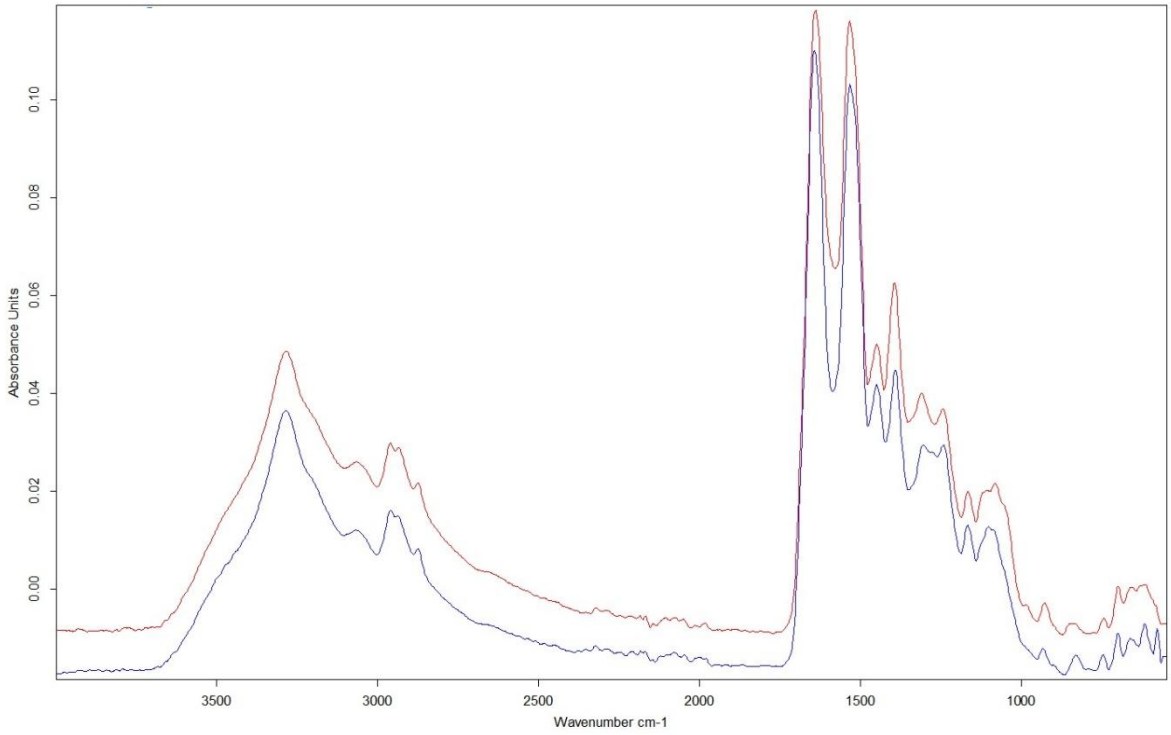


Fig. 3 - Overlaid ATR FT-IR spectra of ante-mortem (blue) and post-mortem (red) blood

As shown in the spectral profiles of ante-mortem and post-mortem blood, they are visually indistinguishable **(Fig. 3)**. As a result, visual analysis alone is insufficient to differentiate between these two blood types, given their highly similar spectral characteristics. Therefore, to achieve objective discrimination between ante-mortem and post-mortem blood, it was necessary to employ multivariate statistical analysis methods. As suggested by Takamura et al. [15], a relative absorbance difference at 1127 cm^{-1} was observed between ante-mortem and post-mortem blood samples. However, the corresponding peak was not sufficiently prominent to allow clear visual differentiation between the two classes. Similarly, in the present study, the 1127 cm^{-1} band was not found to be a reliable marker for distinguishing ante-mortem and post-mortem blood samples. The observed spectral variations at this region were subtle and could not be effectively interpreted through direct visual inspection, thereby necessitating the application of chemometric analysis for accurate discrimination.

3.3 Discrimination of ante-mortem and post-mortem blood using Chemometrics

Chemometrics is used to statistically interpret the obtained data from ATR FTIR. Since visual discrimination is ineffective for distinguishing between ante-mortem and postmortem

blood, chemometric methods such as PCA, PLSDA, and LDA are used to identify biochemical constituents in both blood types.

3.3.1 Discrimination of Ante-mortem and Post-mortem Blood Samples using PCA model

In this study, PCA was conducted on spectral data obtained from both ante-mortem and postmortem blood samples. The results of the PCA for classifying the two types of blood based on their spectral profiles are illustrated in **Fig. 4**. The analysis revealed that the first three principal components (PCS), with PC-1 being the most prominent, were sufficient to achieve 100% classification accuracy; no misclassifications were observed in the dataset. This finding indicates that the PCA model was effective for distinguishing between ante-mortem and post-mortem blood using the analysed spectral data. PC-1 accounted for most of the variance in the dataset and demonstrated a clear separation between samples. Ante-mortem samples consistently exhibited positive PC-1 scores, while post-mortem samples were clustered at negative PC-1 values. Scores along PC-2 were tightly clustered around zero for both sample groups, suggesting that this component captures minor within-group variability.

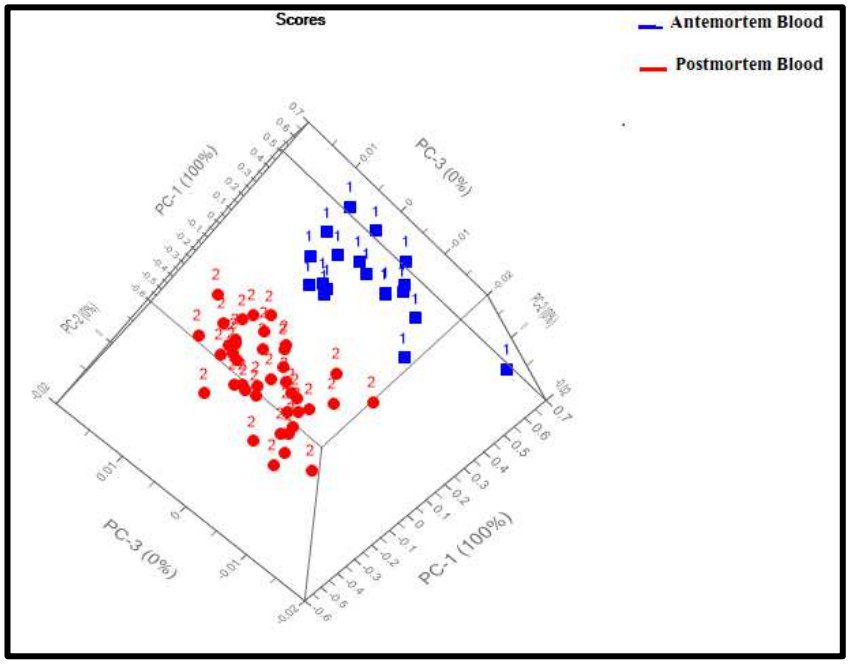


Fig – 4 PCA Model for Ante-mortem and Post-mortem Blood

3.3.2 Interpretation of PCA Results

PCA was performed to evaluate the overall structure of the dataset and to identify potential outliers. The PCA model was assessed using a Hotelling's T^2 vs. Q-residuals (F-residuals)

plot, which evaluates both the leverage of samples in the model space and the variance not explained by the principal components **(Fig. 5)**

Most samples clustered well within the Hotelling's T^2 confidence limit (vertical red line) and below the Q-residual (F-residual) threshold (horizontal red line). This indicates that the majority of samples are adequately described by the PCA model and conform to the dominant variance structure captured by PC-1.

A small number of samples exhibited relatively higher Hotelling's T^2 values, suggesting increased leverage along PC-1. However, these samples remained below the critical threshold, indicating that they represent natural variation within the dataset rather than true multivariate outliers. Importantly, none of the samples exceeded the Q-residual limit, demonstrating that there is no substantial unexplained variance and that the PCA model provides a good overall fit. These findings support the robustness of the PCA model.

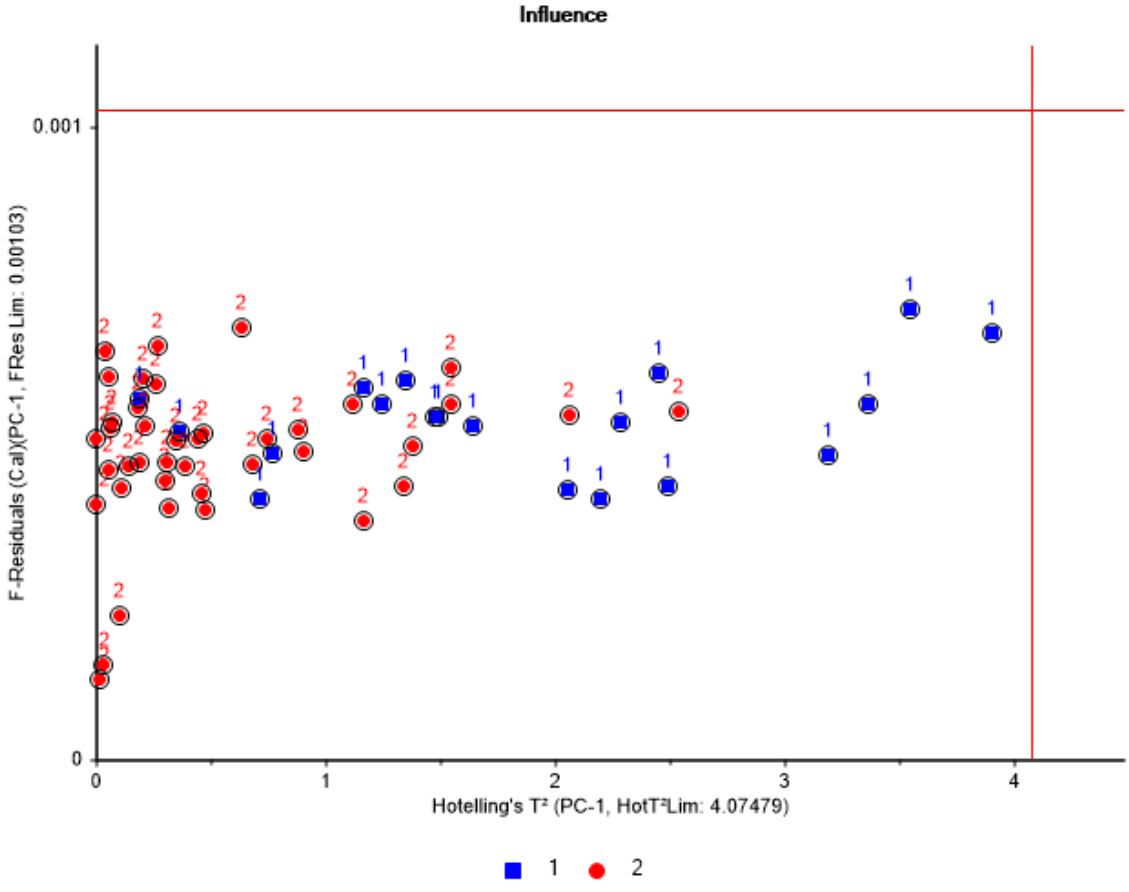


Fig. 5 Hotelling's T^2 vs. Q-residuals plot showing that all samples fall within the 95% confidence limits, indicating good model fit and absence of multivariate outliers.

Fig 6 shows the PCA prediction curve. The PCA prediction curve illustrates the explained variance achieved by the Principal Component Analysis model. This curve clearly indicates that the PC-1 accounts for 100% of the variance in the dataset. Consequently, no additional principal components are necessary for the analysis, as PC-1 alone is sufficient to provide an accurate representation of the variance present. This demonstrates the effectiveness and self-sufficiency of PC-1 in capturing the essential information required from the data. **Fig. 7** shows the PCA loading plot, which illustrates that most of the components show a negative correlation.

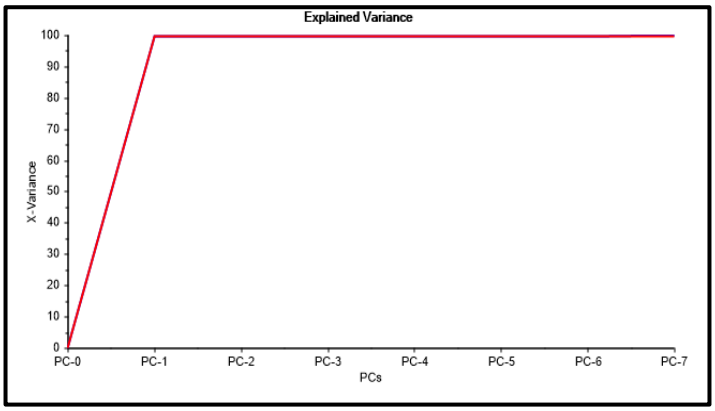


Fig. 6 PCA prediction curve

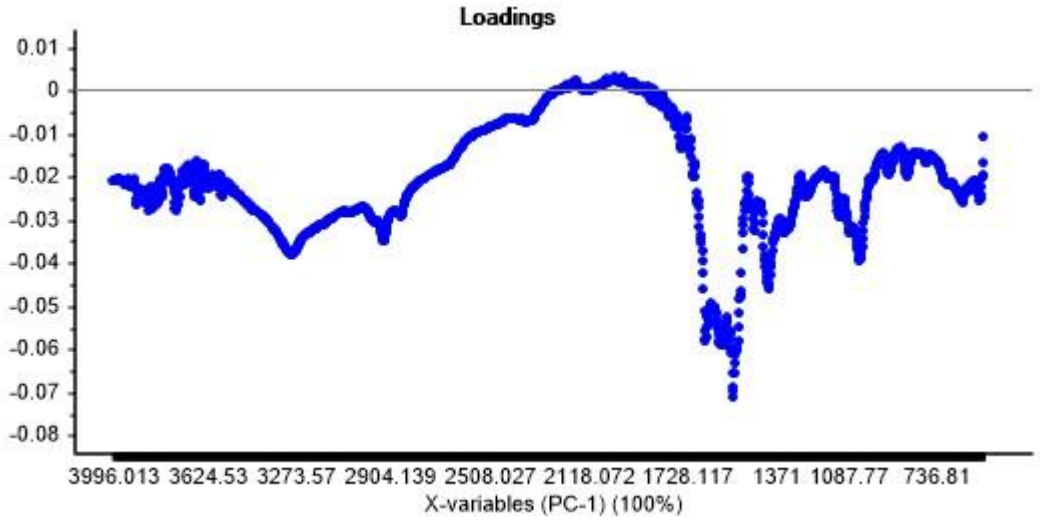


Fig 7 PCA Loading plot

3.4 PLS-DA Model for Sample Discrimination

The PLS-DA model was employed to distinguish between the ante-mortem (Class 1) and post-mortem samples (Class 2). The PLS-DA scores plot constructed using the first three latent variables (Factor-1, Factor-2, and Factor-3) is presented in **Figure 8.** Each point in the plot represents an individual sample, while the axes correspond to the extracted latent variables. In this analysis, Factor 1 accounted for 100% and 83% of the variance within the dataset along the X and Y axes, respectively. Factor 2 explained an additional 7% of the variance along the Y axis, while Factor 3 contributed to 3% of the variation along the Y axis. A clear separation between ante-mortem and post-mortem samples is observed primarily along Factor-1. Ante-mortem samples are predominantly located on the negative side of Factor-1, whereas post-mortem samples cluster on the positive side, indicating that Factor-1 contains the majority of the class-discriminating information. This strong separation demonstrates the ability of the PLS-DA model to effectively differentiate between the two sample classes. **Factors 2 and 3** exhibit relatively small score values and do not contribute significantly to class separation. These factors mainly describe minor variations within each class rather than between classes.

The limited overlap between ante-mortem and post-mortem samples suggests low misclassification and good model robustness. Overall, the observed clustering pattern confirms the reliability and discriminatory power of the PLS-DA model. The classification of samples was performed with high precision according to the biochemical components present in the blood, with no misclassifications observed. R-squared values for the samples were determined by classification, and the resulting model was used to differentiate effectively between the ante-mortem and post-mortem blood. The PLSDA model successfully assigned all samples to their respective predefined classes of ante-mortem and post-mortem blood, achieving an accuracy rate of 100% with 0% false positive and negative rates in classifying the samples. **Table 2** shows the accuracy of discriminating between ante-mortem and post-mortem blood.

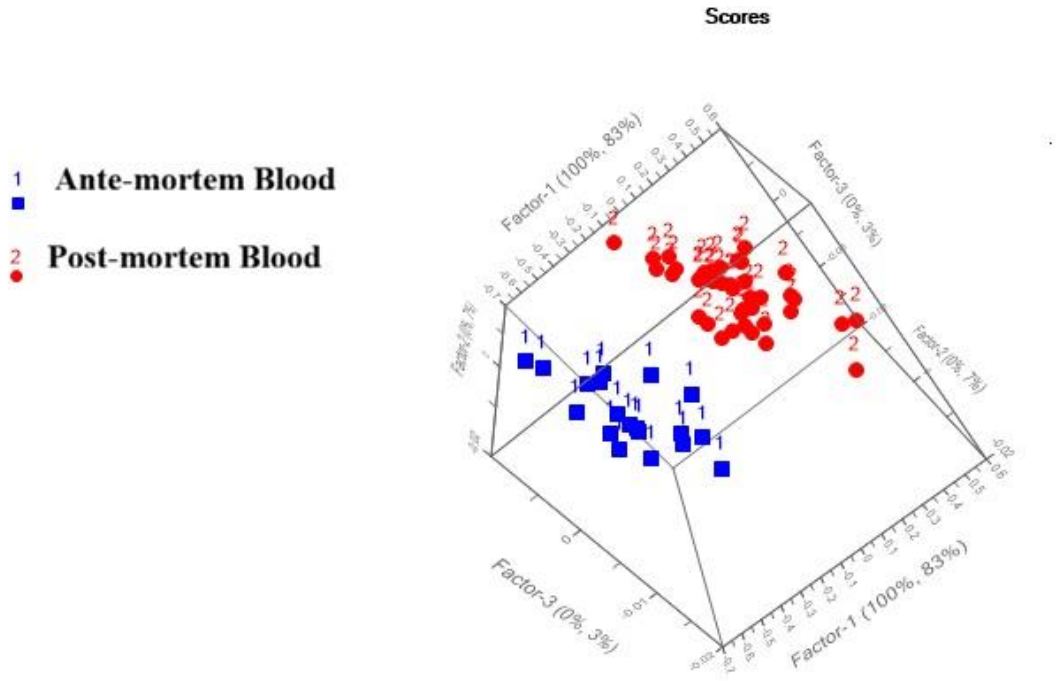


Fig. 8 PLS-DA model of both blood types

Table 2 – Accuracy table for differentiating blood types using PLSDA model

	Ante-mortem Blood	Post-mortem Blood	Correct Classification	Misclassification
Ante-mortem Blood	20	0	100%	0%
Post-mortem Blood	0	40	100%	0%

3.4.1 Model Performance and Selection of Latent Variables

The PLS-DA model demonstrated a consistent improvement in classification accuracy as the number of latent variables, or factors, was increased. The calibration accuracy, the measure of how well the model fits the data used during its construction, reached as high as 97.9% when seven factors were included. However, the validation accuracy, which reflects the model's performance on new, unseen data, plateaued at around 90%. This divergence between calibration and validation accuracy beyond four latent variables suggests the onset

of overfitting, where the model becomes too tailored to the training data and loses its generalisability. Calibration refers to the use of data that was available and used to build the model. In contrast, validation involves testing the model with new, previously unseen data, providing a realistic measure of its reliability in practice. At zero factors (**Factor-0**), the model was unable to perform any classification, resulting in 0% accuracy. As the number of latent variables increased, the accuracy improved for both calibration and validation sets. Calibration accuracy rose sharply, approaching 98% with higher numbers of factors. Validation accuracy also improved, albeit more gradually, stabilising at nearly 90% (**Table 3 and Fig 9**). Based on the observed trends, the optimal model configuration was determined to be three or four latent variables.

Table 3 Classification accuracy (%) of the PLS-DA model for calibration and validation datasets using different numbers of factors.

Number of Factors	**Factor-0**	**Factor-1**	**Factor-2**	**Factor-3**	**Factor-4**	**Factor-5**	**Factor-6**	**Factor-7**
Calibration	0.00	82.95	90.27	93.18	95.97	96.80	97.34	97.94
Validation	0.00	82.27	85.59	85.66	87.38	87.38	88.17	89.84

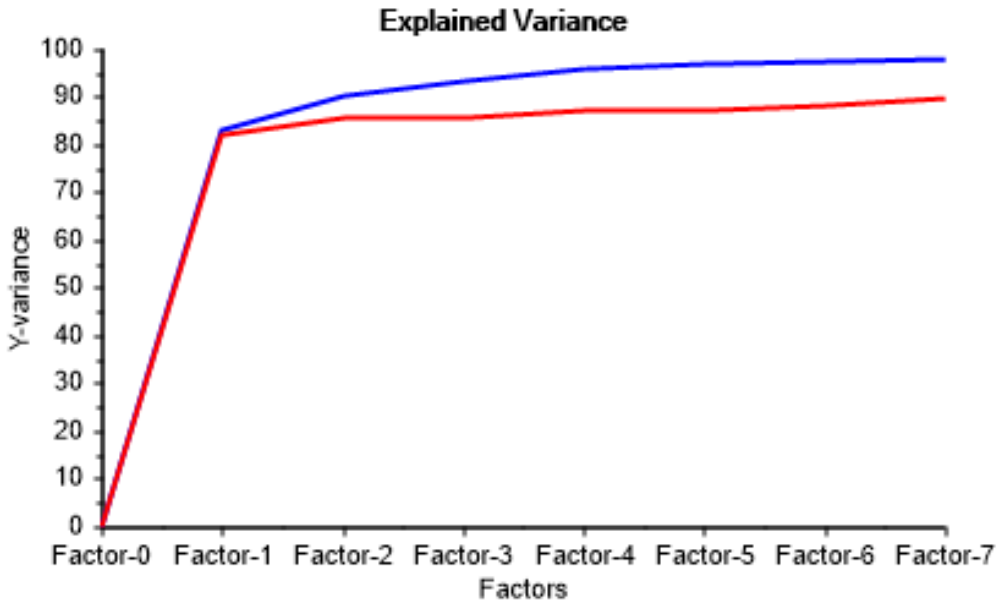


Fig.9 Calibration (Red) and validation (validation) performance of the PLS-DA model

3.4.2 Predicted Versus Reference Plot

The predicted versus reference plot serves to compare the actual class values of the samples with those predicted by the PLS model (Fig. 10). The reference (actual) values represent the true class assignments, where 1 corresponds to ante-mortem samples, and 2 corresponds to post-mortem samples. The predicted values are those generated by the PLS model for each sample, providing an assessment of the model's accuracy in classifying the samples.

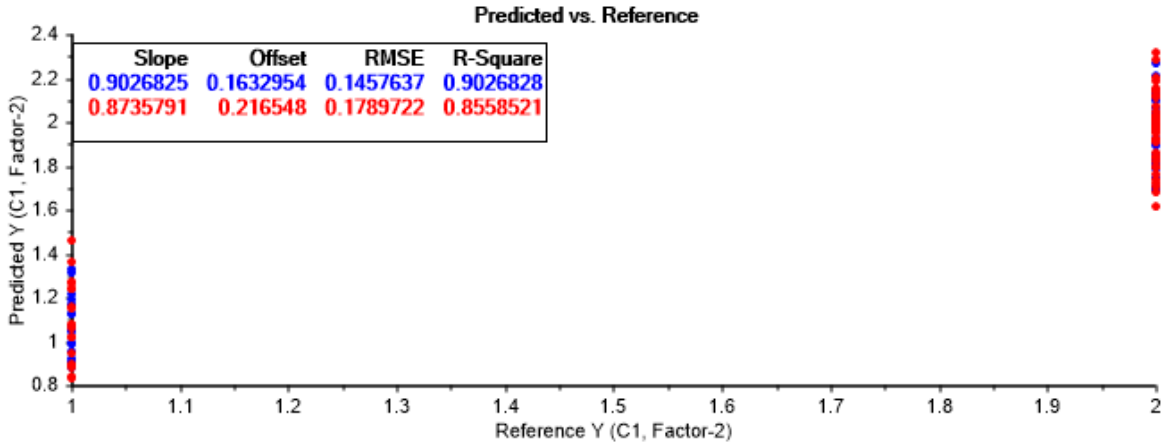


Fig. 10 Predicted versus reference values for the PLS model showing calibration (blue) and validation (red) results. The strong linear relationship, high R^2 values, and low RMSE indicate good agreement between predicted and actual class value

The slope values obtained are 0.90 (blue, calibration) and 0.87 (red, validation). A slope close to 1 indicates strong agreement between predicted and reference values. These results demonstrate a good linear relationship. The offsets are 0.16 and 0.22. Ideally, an offset near 0 suggests no major systematic error in the predictions. The small offsets observed here confirm that the PLS model does not introduce significant bias. The RMSE (Root Mean Square Error) values are 0.15 (blue) and 0.18 (red). Lower RMSE values reflect better predictive performance. The low RMSE values observed indicate minimal prediction errors. The R-Square (R^2) values close to 1 suggest a strong correlation between predicted and actual values, providing further evidence of the model's reliability.

Reference values are assigned as 1 for Ante-mortem samples and 2 for post-mortem samples. The predicted values closely correspond to these reference values, with only minor deviations (e.g., 1.12, 1.90, 2.14), which are considered normal and acceptable in classification tasks. Very few data points deviate significantly from their true class, indicating good classification performance by the PLS model.

The predicted versus reference plot clearly demonstrates strong agreement between actual and predicted values for both Ante-Mortem and Post-Mortem samples. The high R^2 values and low RMSE confirm that the PLS model is capable of accurately predicting sample classes, with only minor deviations from the reference values. Fig 11 presents the factor loading plot for Factor 1 of the PLS-DA model. The analysis revealed that few negative peaks are observed exclusively within the wavenumber region from 2212.482 cm^{-1} to 1830.737 cm^{-1}. In contrast, significant positive peaks are noted around the wavenumber intervals ranging from 3996.013 cm^{-1} to 2407.46 cm^{-1} and also from 1830.737 cm^{-1} down to 648.557 cm^{-1}. These findings highlight the specific spectral regions that are influential in distinguishing between the blood types in the model. The model shows good discrimination ability, as validation accuracy consistently improves.

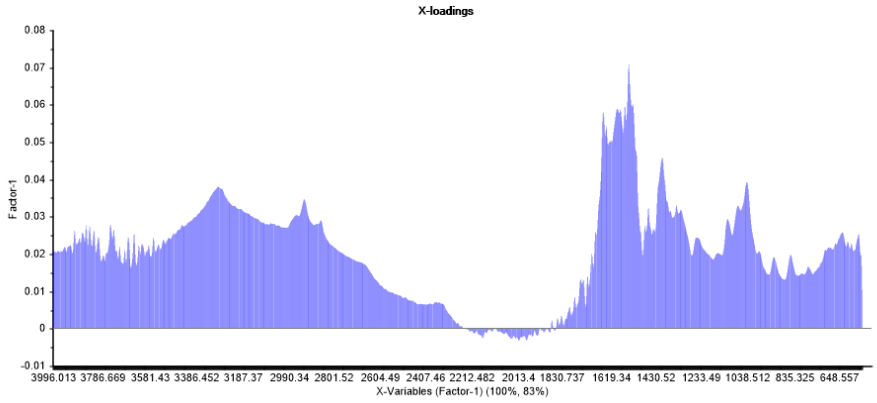


Fig 11 PLSDA Factor loadings to differentiate between ante-mortem and post-mortem blood

3.5 Classification of Ante-mortem and Post-mortem Blood Samples Using LDA Models

The differentiation between ante-mortem and post-mortem blood samples was achieved through a four-component analysis. In this approach, the samples were categorised into two distinct classes: ante-mortem blood and post-mortem blood. The classification relied on both the linear LDA (Linear Discriminant Analysis) model and the Mahalanobis-LDA model to rigorously assess the accuracy of discrimination between these two groups.

The linear LDA model demonstrated a good classification performance, achieving an overall 100% correct classification rate. This means that all samples were correctly identified as

either ante-mortem or post-mortem based on their respective characteristics. The robustness of the classification was further validated by the Mahalanobis-LDA model, which provided additional confirmation of the model's effectiveness in distinguishing between the groups. Visual representations of the classification results are provided in **Fig. 12** for the linear LDA model and **Fig. 13** for the Mahalanobis-LDA model.

Linear Discriminant Analysis projects multivariate data into a reduced-dimensional space, optimising the separation between predefined groups while minimising variance within each group. The first linear discriminant (LD1) accounted for the majority of the between-group variation, clearly segregating ante-mortem and post-mortem samples. Ante-Mortem samples were grouped at higher LD1 values, whereas PM samples clustered at lower LD1 scores. The second linear discriminant (LD2) explained a comparatively smaller proportion of the variance and mainly reflected within-group heterogeneity rather than group separation. Replicate samples were found to cluster closely together in the LD1 and LD2 space, demonstrating both analytical reproducibility and consistency of measurements. A few PM samples exhibited more extreme LD1 values, indicating greater variability within the PM group. The results of LDA showed the 100% sensitivity, selectivity, specificity, accuracy and 0% false positive and 0% false negative results were obtained.

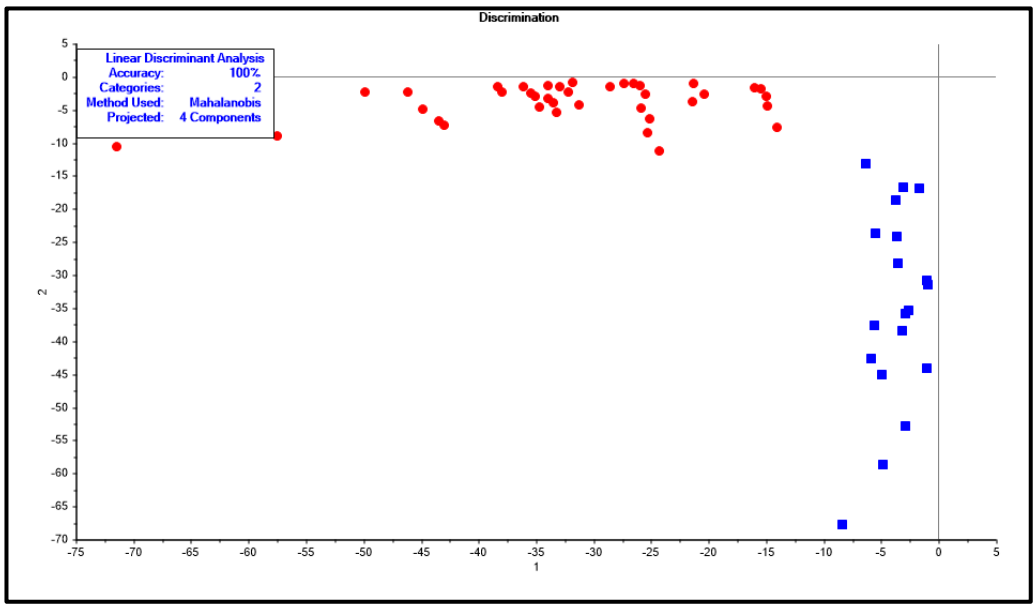


Fig 12 – Linear- LDA model

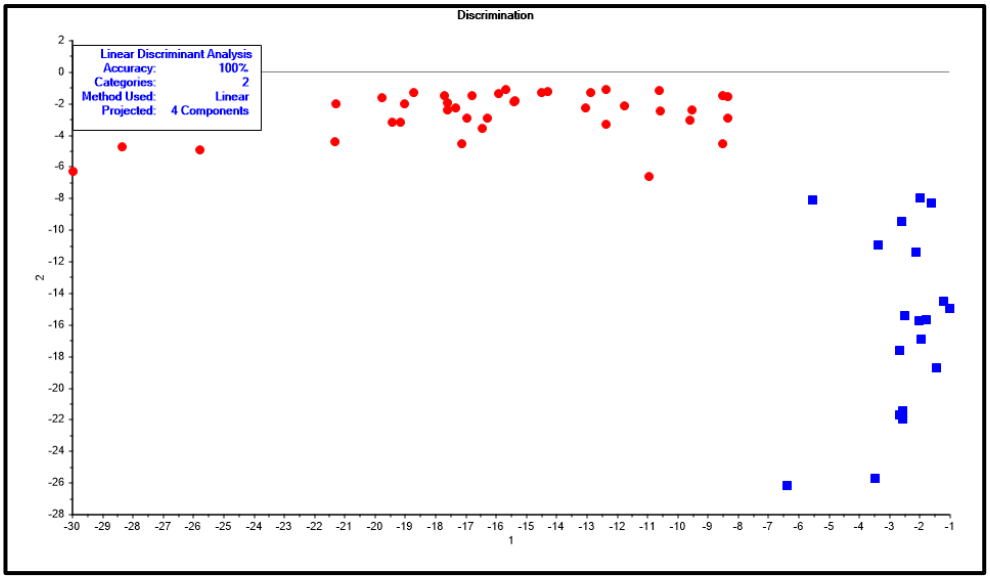


Fig. 13 Mahalanobis-LDA model.

4. Effects of substrates on the Ante-mortem and Post-mortem Blood

Analysis of the overlaid comparative spectra for neat post-mortem blood and post-mortem blood deposited on various substrates shows that there are no significant differences observed between the samples. The spectral peaks corresponding to amides, lipids, and CH_3 bending (both symmetric and asymmetric) remain consistent across all tested substrates. This observation indicates that the chemical features of these biomolecules are preserved, regardless of the substrate on which the blood is deposited. Notably, any observable effects are most prominent in the region beyond 1000 cm^{-1}, where substrate influence becomes more apparent (Fig. 14-17).

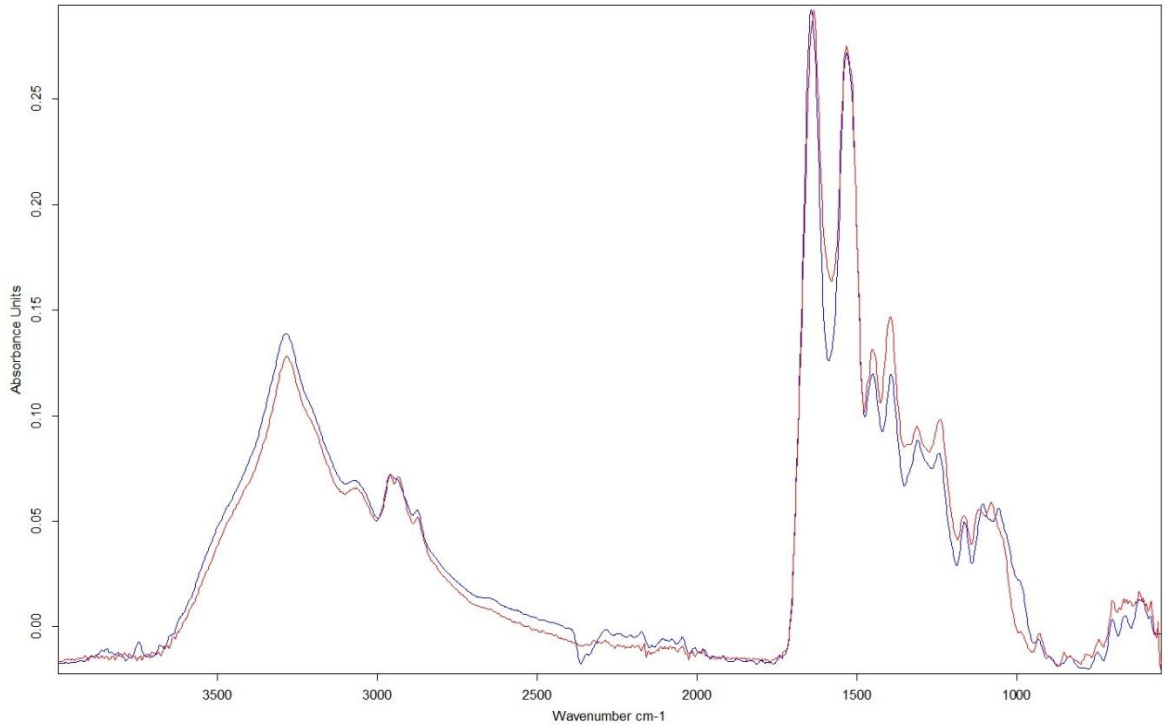


Fig:14 Overlaid spectra of post-mortem blood deposited on cotton cloth (blue) and neat post-mortem blood (red)

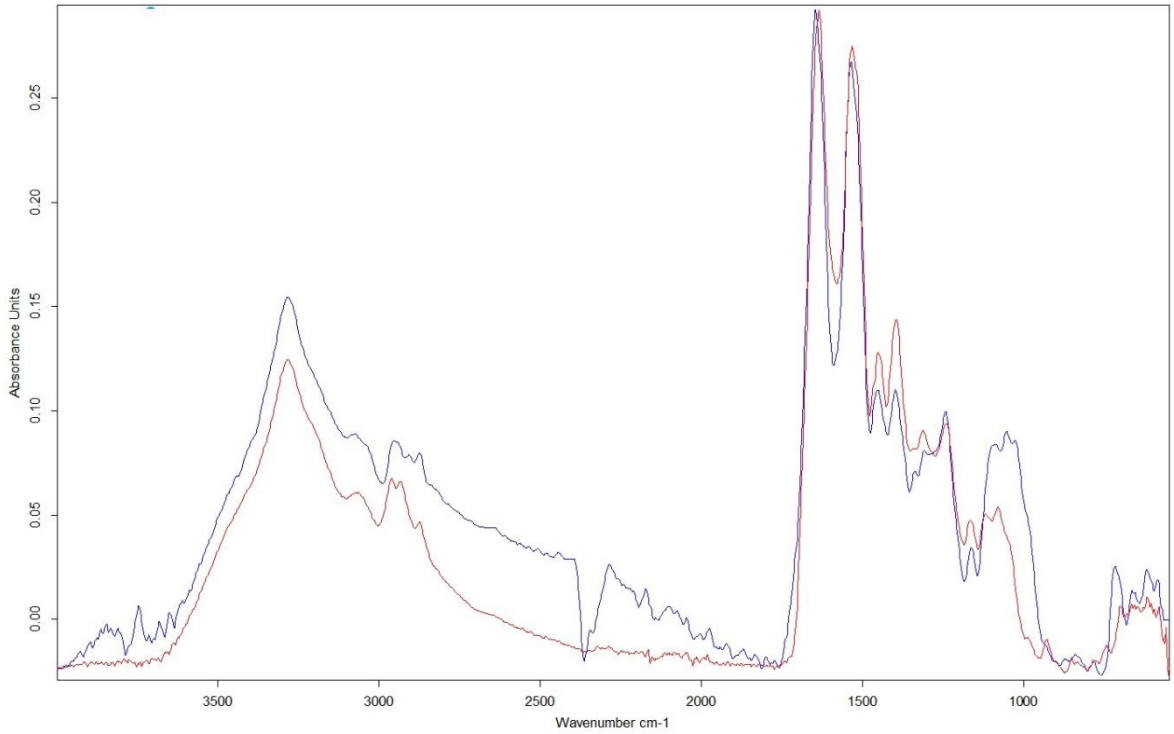


Fig 15 Overlaid spectra of post-mortem blood deposited on single fiber (blue) and neat post-mortem blood (red)

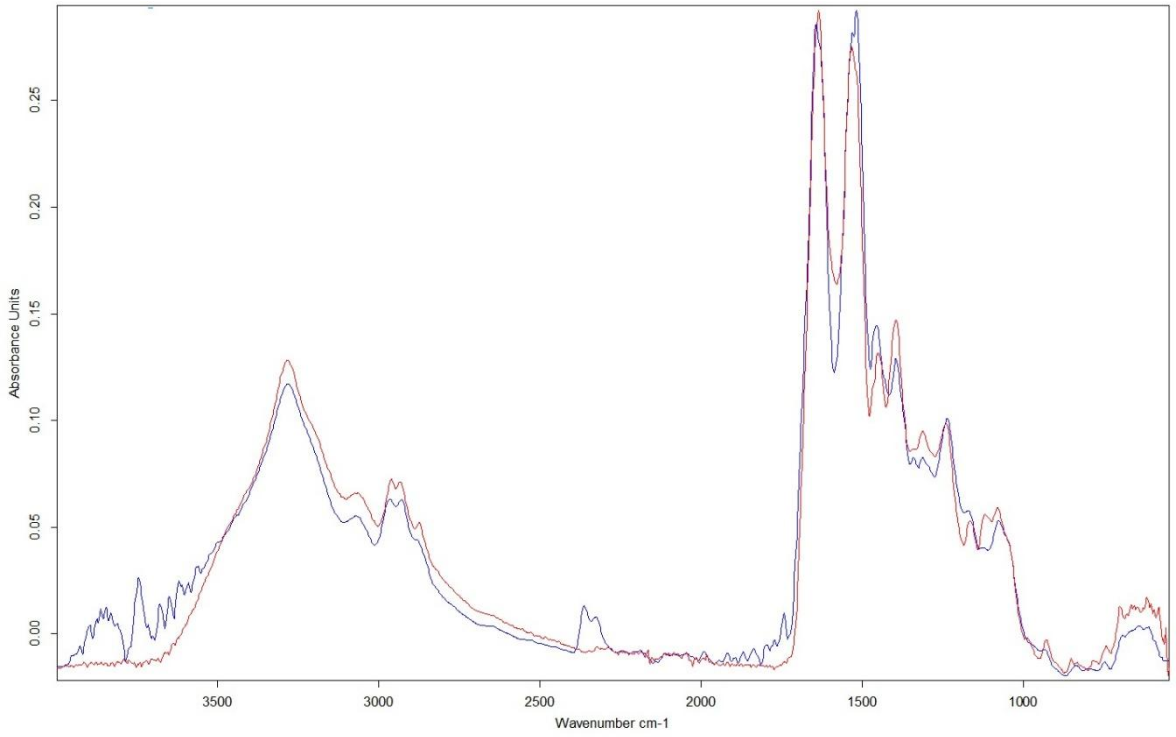


Fig 16 Overlaid spectra of post-mortem blood deposited on hair (blue) and neat post-mortem blood (red)

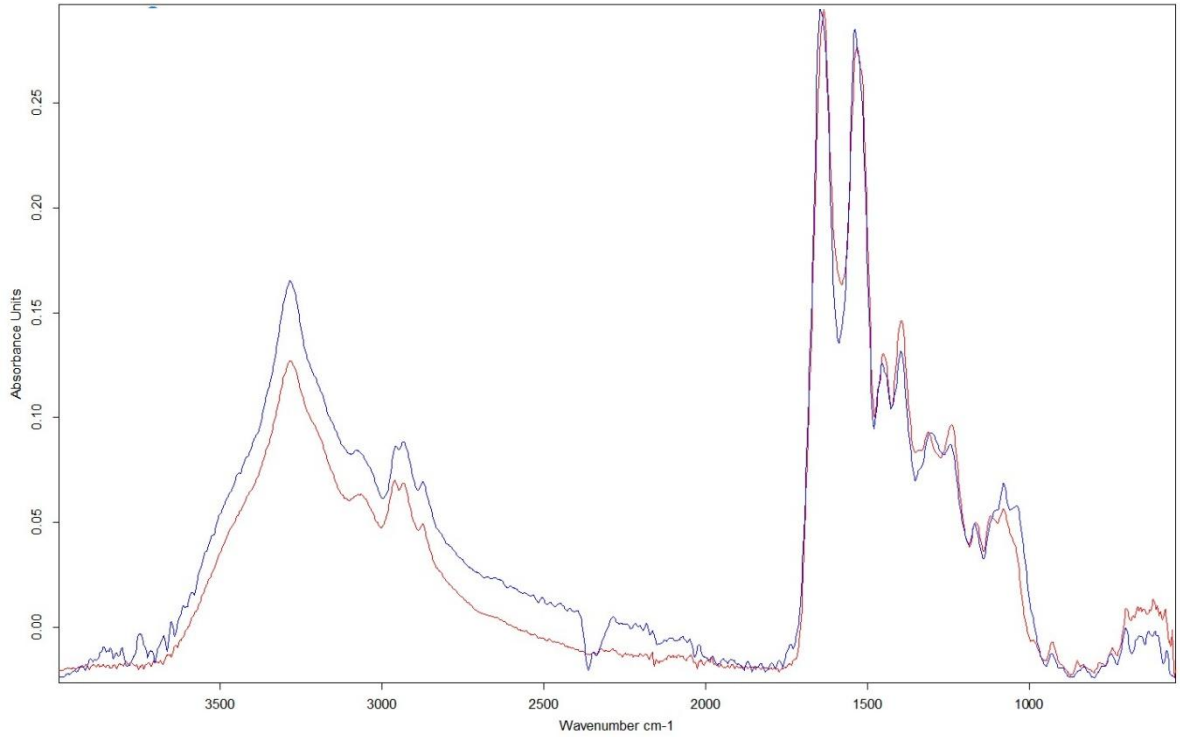


Fig 17 Overlaid spectra of post-mortem blood deposited on nail (blue) and neat post-mortem blood (red)

5. Effect of storage and non-storage conditions for Post-mortem Blood Samples

After death, biological samples such as blood undergo various biochemical and cellular changes. These include enzymatic degradation, protein denaturation, and cell lysis. Such alterations can influence the chemical state of the sample and potentially impact the results of downstream analytical methods. Despite these changes, the biochemical integrity of post-mortem blood can be sufficiently maintained for analysis under certain conditions. Storing post-mortem blood at ultra-low temperatures, typically at –80°C in EDTA, helps to preserve the sample, especially when there is a delay before analysis.

In this study, two types of blood samples were prepared to assess how the presence of EDTA (a chelating agent that prevents clotting and minimises metal ion-catalysed degradation) and storage conditions affect the chemical profile of blood.

Blood was collected from the cardiac region of post-mortem bodies using EDTA vials and then stored at –80°C. EDTA acts by chelating calcium ions, which are essential for the extrinsic, intrinsic, and common pathways of the clotting cascade, as well as for certain

enzymatic reactions. In addition, ultra-low temperature freezing halts all biological and chemical activity, thus preserving the native biochemical profile of the blood.

Another set of samples was prepared by directly smearing blood onto clean glass slides and allowing them to air dry for 24 hours. These samples were neither frozen nor treated with EDTA, representing the "non-stored" condition.

The key observation from the study was that, irrespective of EDTA treatment, no significant spectral differences were observed between dried blood samples that were stored and those that were not (Fig 18). There was no significant difference between the spectra of stored and non-stored blood, indicating that once blood has dried, no further cellular activity occurs.

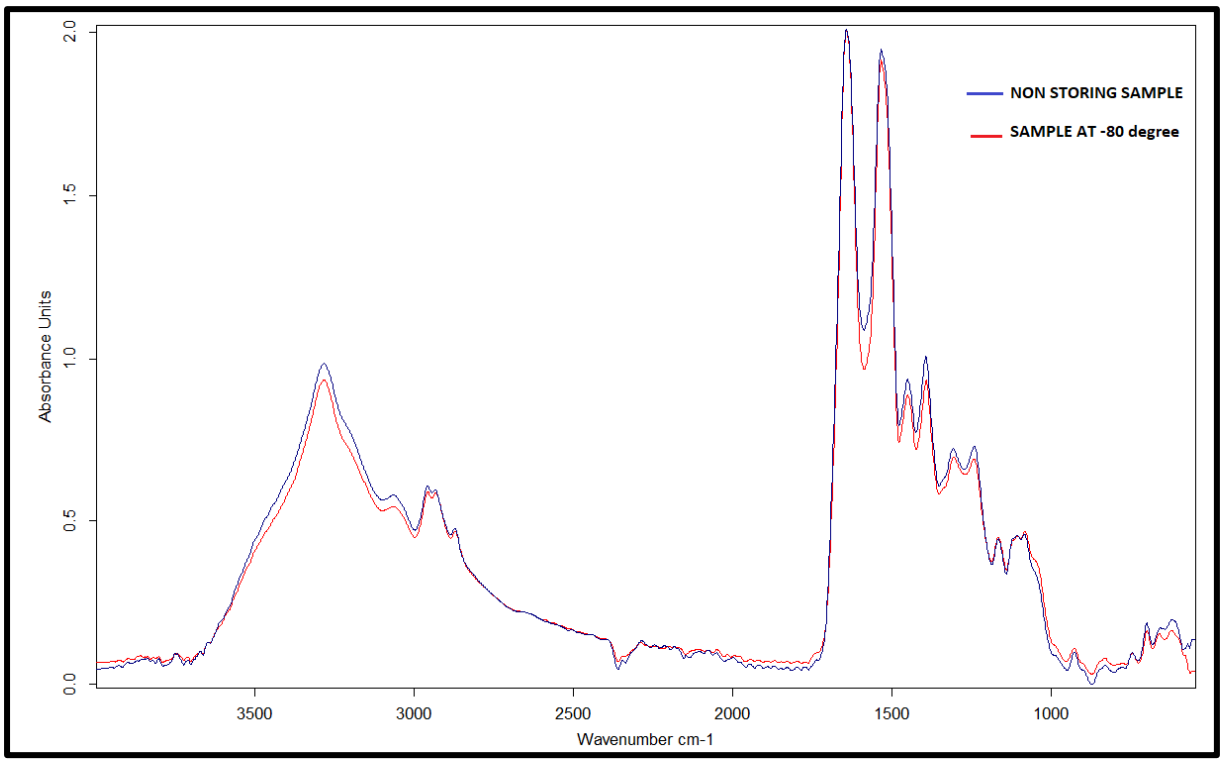


Fig. 18 Overlaid spectra of blood sample stored at room temperature and sample stored at -80°C

5. External Validation

An external validation study was performed to evaluate the robustness, reliability, and predictive performance of the developed chemometric model for the discrimination of menstrual blood (class 1), ante-mortem blood (class 2), and post-mortem blood (class 3) samples. For the external validation study, 10 independent

samples of menstrual blood were collected to discriminate from ante-mortem and post-mortem blood.

The score plot obtained from the external validation study (Figure 19) demonstrated a clear and well-defined clustering pattern for all three classes without any overlap among the groups. Menstrual blood samples formed a distinct cluster separated from both ante-mortem and post-mortem blood samples, while post-mortem blood samples also exhibited complete discrimination from ante-mortem blood. The observed separation indicates significant biochemical variations among the three blood classes, which were successfully captured by ATR-FTIR spectroscopy and chemometric analysis. The model achieved 100% classification accuracy during external validation, with no false positive or false negative classifications observed in any of the three groups (Table 3). The results confirm the robustness and reproducibility of the developed model and demonstrate its potential applicability in forensic investigations, particularly in situations where menstrual blood may create ambiguity during the interpretation of post-mortem blood evidence. As shown in Figure 20, the R^2 value obtained for the classification of menstrual blood from ante-mortem and post-mortem blood is 0.9, suggesting a strong correlation between predicted and actual values.

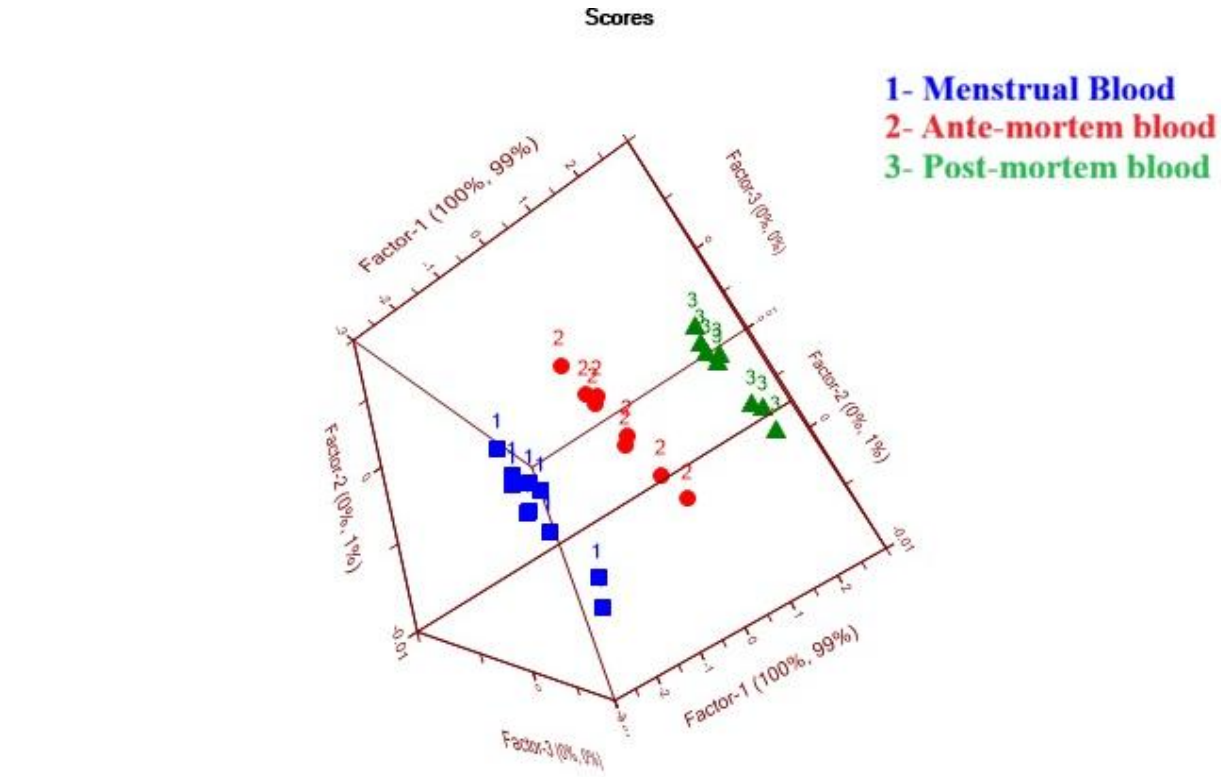


Fig.19 3-D score plot showing the classification of Menstrual blood, Ante-mortem blood and Post-mortem blood

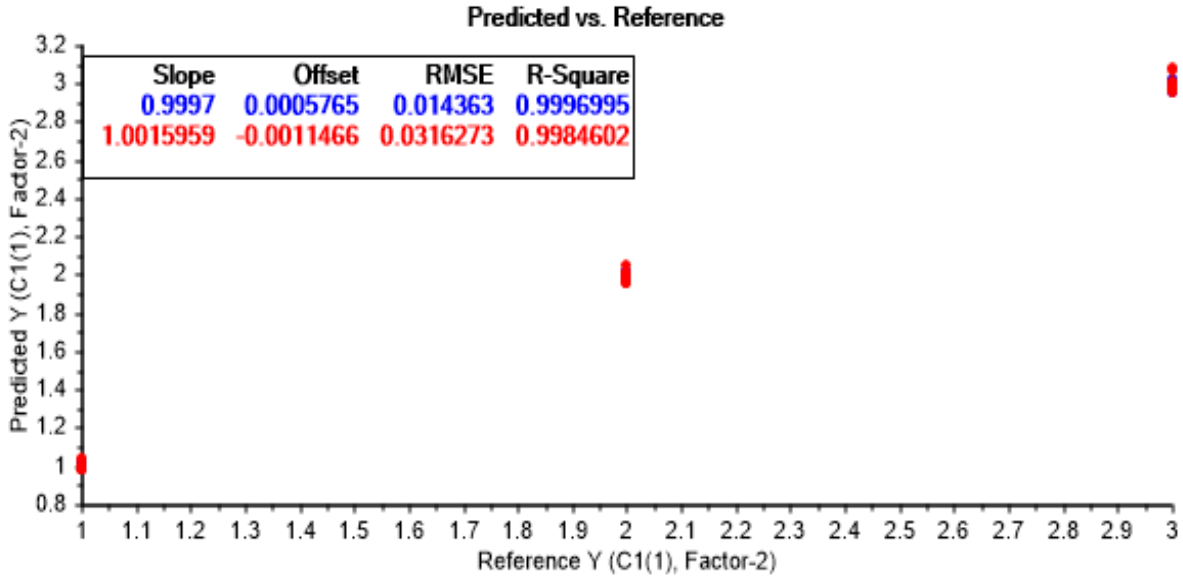


Fig.20 Predicted vs Ref plot for the classification of Menstrual blood, Ante-mortem blood and post-mortem blood

Table 4. External Validation Classification Table of Menstrual blood, Ante-mortem blood and Post-mortem blood

Blood Class	Menstrual Blood **(class 1)**	Ante-mortem Blood (class 2)	Post-mortem Blood (class 3)	**Misclassified**	**False Positive**	**False Negative**	**Classification Accuracy**
Menstrual Blood	10	0	0	0	0	0	100%
Ante-mortem Blood	0	10	0	0	0	0	100%
Post-mortem Blood	0	0	10	0	0	0	100%

7. CONCLUSIONS

The integration of ATR-FTIR spectroscopy with chemometric analysis has emerged as an exceptionally effective, rapid, and non-destructive approach for distinguishing between ante-mortem and post-mortem blood samples. This study was designed to elucidate the biochemical distinctions between blood collected prior to and following death, while also evaluating how various substrates influence the resulting spectroscopic profiles. The findings demonstrate that ATR-FTIR spectroscopy, supported by chemometric techniques, enables clear spectral differentiation between antemortem and post-mortem blood. The application of PCA revealed distinct clustering patterns within the spectral datasets, effectively separating the two blood types. Furthermore, the use of PLS-DA resulted in 100% classification accuracy, confirming the reliability of this method. Additional analyses using Linear-LDA and Mahalanobis-LDA also achieved 100% accuracy, underscoring the robustness of these statistical approaches.

The study further evaluated the influence of different substrates, including cotton cloth, single fibre, hair, and nail, as well as storage conditions (room temperature and −80°C), on

the spectral characteristics of post-mortem blood samples. The developed ATR-FTIR chemometric models demonstrated robust and reliable classification performance irrespective of substrate interference or storage variation. Moreover, external validation successfully discriminated menstrual blood from ante-mortem and post-mortem blood with 100% classification accuracy, highlighting the potential of the proposed approach as a rapid, non-destructive, and highly reliable tool for forensic blood identification and differentiation.

Statements and Declarations

Competing Interests:

The authors have no competing interests to declare that are relevant to the content of this article.

Consent to Participate

Informed consent was obtained from all individual participants included in this study. Participation was voluntary, and all participants provided written informed consent prior to sample collection and analysis. For the collection of antemortem samples, all participants were informed about the study, and their consent were duly recorded. Informed consent for the collection of post-mortem samples was obtained from the next of kin of the deceased.

Ethics Approval

All procedures performed in this study involving human participants were in accordance with the Institutional Ethical Committee (NFSU-DC/EC/005/2025).

Funding Declaration

The authors did not receive support from any organization for the submitted work.

Conflict of Interest

The authors declare no conflict of interest and confirm that there are no personal or financial relationships that could influence the present study.

Declaration of Generative AI Use

During the preparation of this manuscript, Microsoft Copilot (integrated within Microsoft Word) was used solely to assist with structuring, language refinement, and improvement of clarity and readability of the text. The scientific content, study design, data generation, analysis, interpretation, and conclusions are entirely original and were conducted by the authors.

References

[1] S. Sharma, R. Chophi, J.K. Jossan, R. Singh, Detection of bloodstains using attenuated total reflectance-Fourier transform infrared spectroscopy supported with PCA and PCA–LDA, Med. Sci. Law. (2021) 00258024211010926.

[2] K. Virkler, I.K. Lednev, Analysis of body fluids for forensic purposes: From laboratory testing to non-destructive rapid confirmatory identification at a crime scene, Forensic Sci. Int. 188 (2009) 1–17. https://doi.org/https://doi.org/10.1016/j.forsciint.2009.02.013.

[3] F. Zapata, M. Silva Gregório Martins, C. García-Ruiz, Body Fluids and Spectroscopic Techniques in Forensics: A Perfect Match?, 2015. https://doi.org/10.4172/jfm.1000101.

[4] S. Sharma, R. Chopi, R. Singh, Forensic characterization of menstrual blood and peripheral blood using Attenuated Total Reflectance (ATR) - Fourier Transform Infrared (FTIR) Spectroscopy and chemometrics, Int. J. Legal Med. (2019). https://doi.org/10.1007/s00414-019-02134-w.

[5] C.-M.R. Orphanou, A BIOANALYTICAL APPROACH TO FORENSIC BODY FLUID IDENTIFICATION & AGE DETERMINATION, Staffordshire University, 2015. https://pdfs.semanticscholar.org/e033/3b2bf1fad58ce522ccdb5b6f522b1bf52890.pdf.

[6] R. Hauser, G. Fechner, B. Brinkmann, Differentiation between in-life and post-mortem hemorrhage, Beitr. Gerichtl. Med. 48 (1990) 437–441.

[7] M. Hashimoto, M. Fujishiro, A. Nakauchi, H. Sone, S. Minohara, N.M. Jui, Y. Tachi, K. Sato, T. Onizuka-Yamochi, T. Matsuyama, Methemoglobin concentration for the distinction between antemortem thrombus and postmortem coagulation, Showa Univ. J. Med. Sci. 34 (2022) 102–110.

[8] K. Kibayashi, T. Higashi, S. Tsunenari, A differential study between antemortem bleeding and a postmortem infiltration of hemoglobin., Nihon Hoigaku Zasshi= Japanese J. Leg. Med. 45 (1991) 227–232.

[9] S. Miyaishi, F. Moriya, Y. Yamamoto, T. Kitao, H. Ishizu, Discrimination between

postmortem and antemortem blood by a dot-ELISA for human myoglobin., Nihon Hoigaku Zasshi= Japanese J. Leg. Med. 48 (1994) 433–438.

[10] D. Morena, A.M. Manta, A. Santurro, M. Scopetti, E. Turillazzi, V. Fineschi, Bloody Evidence: The Validity of Glycophorin A in the Determination of Wound Vitality—A Systematic Review of the Literature, Int. J. Mol. Sci. 26 (2025) 5308.

[11] S. Sharma, R. Singh, Detection of vaginal fluid stains on common substrates via ATR FT-IR spectroscopy, Int. J. Legal Med. 134 (2020) 1591–1602.

[12] S. Sharma, R. Singh, Detection and discrimination of seminal fluid using attenuated total reflectance Fourier transform infrared (ATR FT-IR) spectroscopy combined with chemometrics, Int. J. Legal Med. (2019) 1–22.

[13] E. Mistek-Morabito, I.K. Lednev, Discrimination of menstrual and peripheral blood traces using attenuated total reflection Fourier transform-infrared (ATR FT-IR) spectroscopy and chemometrics for forensic purposes, Anal. Bioanal. Chem. (2021). https://doi.org/10.1007/s00216-021-03206-w.

[14] E. Mistek, I.K. Lednev, Identification of species' blood by attenuated total reflection (ATR) Fourier transform infrared (FT-IR) spectroscopy, Anal. Bioanal. Chem. 407 (2015) 7435–7442. https://doi.org/10.1007/s00216-015-8909-6.

[15] A. Takamura, K. Watanabe, T. Akutsu, H. Ikegaya, T. Ozawa, Spectral Mining for Discriminating Blood Origins in the Presence of Substrate Interference via Attenuated Total Reflection Fourier Transform Infrared Spectroscopy: Postmortem or Antemortem Blood?, Anal. Chem. 89 (2017) 9797–9804. https://doi.org/10.1021/acs.analchem.7b01756.